Armenian Journal of Physics, 2018, vol. 11, issue 4, pp. 241-245

Plasmonic Nanoparticles Arrangements for Biosensing

(Proceedings of the Int. Conference on " Microwave and THz Technologies and Wireless comm.")

H. Parsamyan, T. Yezekyan, H. Haroyan.
Yerevan State University, 1 Alex Manoogian, 0025 Yerevan, Armenia

Received 15 November 2018

Abstract: The localized surface plasmon resonance (LSPR) of gold and silver spherical and cubic nanoparticles (NP), as well as NP dimers is studied. We use numerical simulations based on finite element method to derive extinction cross sections (ECS) and LSPR wavelengths of the investigated structures. Study of the dependence of the LSPR of the cubic NPs on the different values of chamfering radius shows the red shift of the resonant wavelength while decreasing the chamfering radius. For the silver nanocube the analysis suggests three extinction peaks on ~333 nm, ~364 nm due to strong absorption and on ~400 nm due to scattering, while for gold nanocube there is only one extinction peak on ~526 nm. The diameter of the spheres and the sides of the cubes is 50 nm. According to the simulations the localized surface plasmon properties of the silver nanoparticles are much stronger and more diverse than that of corresponding gold nanoparticles. The study of nanocube and nanosphere dimers is carried out as well.

Keywords: Surface plasmon, plasmonic nanoparticles, biosensing, finite element method.

1. Introduction

The need for a fast, ultracompact, highly-sensitive, label-free and reliable devices for biosensing has provided a growing interest [1]. During the past decades, with the developing of nanotechnology the metal nanoparticles with different morphology have become of great interest due to their unique ability to interact with the incident light causing localized surface plasmon resonance (LSPR) phenomenon. The LSPR is a result of collective oscillations of the free electrons of a metal, which typically appear in the visible or near infrared for noble metals and strongly depends on the material of the particle, shape, sizes and the surrounding medium. These features allow one to use plasmonic metal NPs for study of fundamental optical processes, such as absorption, scattering and non-linear effects [2], as well as for technical applications, including drug delivery [3], cancer therapy [4], electronics, high-resolution imaging [5], surface enhanced Raman spectroscopy [6]. Moreover, the ability of NPs to interact with single small molecules with fluorescence enhancement and confine electromagnetic energy within small volumes make metal NPs good candidates for label-free chemical and biological sensing techniques offering sensitive, robust, and facile detection [7]. The sensing principle relies on the measurements of the LSPR spectral shift caused by the change of surrounding dielectric environment during a binding process. Since the nanoparticles themselves are colored, detection can often be carried out with the naked eye, yielding rapid, portable detection. In addition, the production and fabrication of nanoparticles, which contain small amounts of material, is often inexpensive.

Further advances in nanofabrication techniques led to wide investigation of NPs with various morphologies from nanocubes to more extraordinary structures, such as nanostars and nanotriangles [8-9]. A higher near-field enhancement and strong LSPR features can be achieved

in the structures containing two (dimers) or more closely spaced particles, which distance is in the order of NPs sizes. Thus, plasmonic properties of such systems can be drastically enhanced by exciting the system with a plane electromagnetic wave polarized along the interparticle axis.

This paper is focused on improvement of LSPR biosensors by using different geometries and arrangements of nanoparticles. Here, we present the numerical analysis of the LSPR of the single gold (Au) and silver (Ag) nanoparticles (NP) of spherical and cubic shapes, and for nanoparticle dimers as well. To have a LSPR in visible region, the diameter of the spheres and the sides of the cubes were chosen $50nm$. The optical extinction spectra of the investigated structures are derived via a full wave electromagnetic simulation based on finite element method. Comparative analyses of the extinction cross section ECS (both absorption and scattering cross sections) of the single cubic and spherical NPs, as well as for cube-cube and sphere-sphere NP dimers were carried out.

2. Results and discussion

The first part of simulations is carried out for single silver and gold spherical and cubic NP. During all simulations the diameter of the spheres and the corner size of the cubes were set $50nm$ and chamfering radius was $3nm$. Investigated structures are excited by a plane wave propagating along x-axis and polarized along z-axis. Fig. 1(a) shows the ECS of a single gold nanosphere (black line) and nanocube (red line).

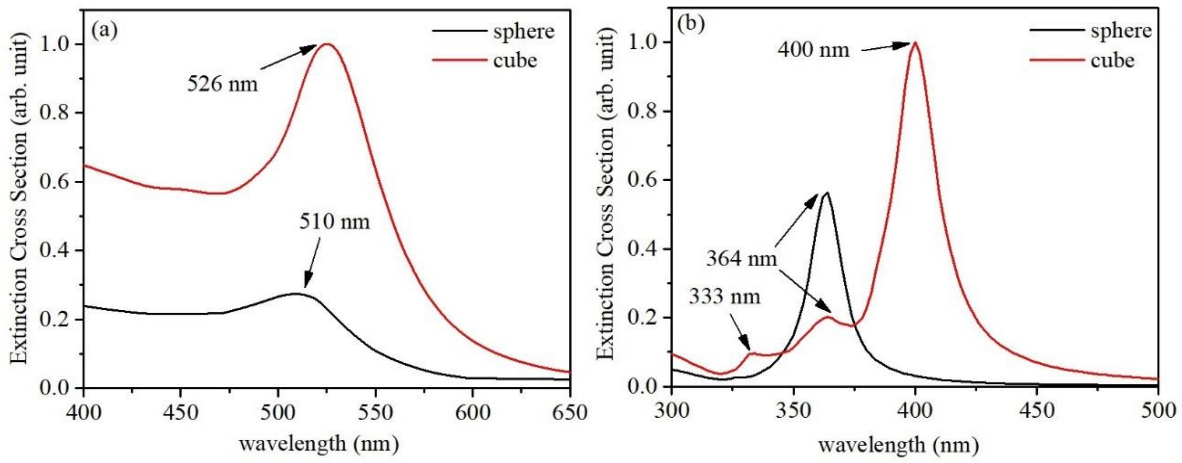

Fig. 1. The Extinction Cross Section of individual (a) gold and (b) silver sphere (black line) and cube (red line).

The extinction peak of the Au sphere is around $510nm$, while for the cube - $526nm$.

The ECS of individual silver nanosphere (black line) and nanocube (red line) are shown on the Fig. 1(b). For the sphere only one extinction peak exists on around $364nm$, while for an Ag cube there are three extinction peaks: around $333nm$ and $364nm$ due to strong absorption and about $400nm$ due to scattering. Note that for both Au and Ag, the plasmonic properties of the cube are much stronger than those of a sphere, which appears because of sharp edges of cubes causing field enhancement around them.

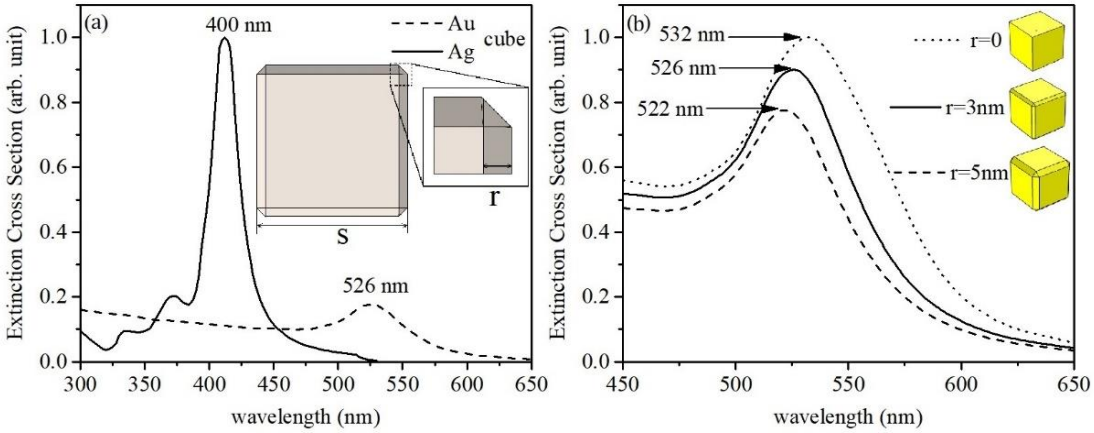

Fig. 2. The Extinction Cross Section of (a) Au (dashed line) and Ag (solid line) cube, (b) individual Au nanocube with different values of the chamfering radius of corners.

Fig. 2(a) shows the comparison of the extinction cross sections of a single Au (dashed line) and Ag (solid line) cubic nanoparticles. The inset of Fig. 2(a) shows the schematic of a single nanocube. The corners of the simulated cubes are chamfered with the radius r (see the zoomed part of Fig 2(a) and inset of Fig. 2(b)). Such morphology corresponds to the dean-flow mixing preparation technique of nanocubes [10]. One can see that the extinction of a silver cube is much higher compared to the gold one. Extinction cross sections of a single Au nanocube of different values of the chamfering radius of corners is presented on Fig. 2(b). The dashed, solid and dotted lines correspond to the chamfering radii of $5nm$, $3nm$ and 0 (ideal cubic shape). The analysis suggests the red shift of the resonant wavelength while decreasing the chamfering radius of a cube.

The second part of simulations includes calculation of the ECS of the simplest case of NP clusters - dimers. The distance between parts of dimers is $5nm$. Fig. 3(a) shows extinction cross sections of spherical (black line) and cubic (red line) Au dimers. According to simulations the LSPR of Au cubic dimer lies around $566nm$, while for spherical dimers - around $528nm$.

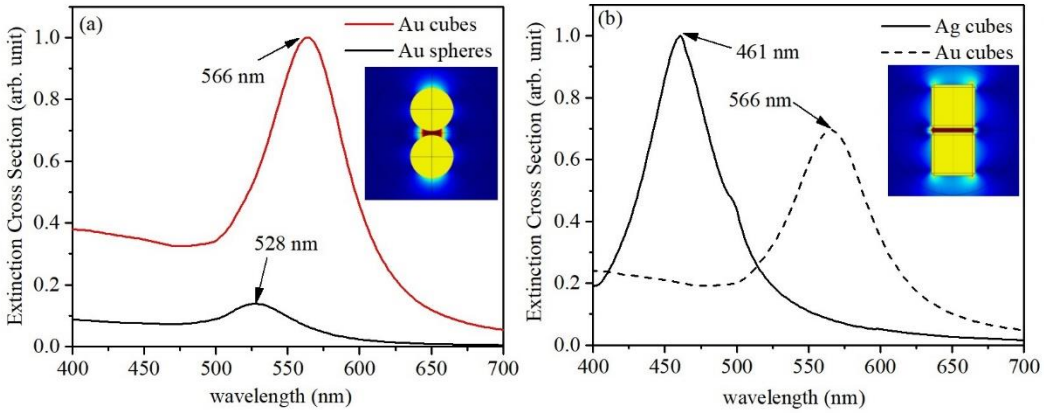

Fig. 3. The Extinction Cross Section of (a) spherical (black) and cubic (red) Au dimers, (b) cubic Ag (solid) and Au (dashed) dimers.

Fig. 3(b) presents the comparison of extinction cross sections of cubic *Au* (dashed line) and *Ag* (solid line) dimers. The resonance of the cubic *Ag* dimer lies around 461 nm. Inset images in Fig. 3(a) and (b) show the field distribution of the spherical and cubic *Au* dimers, respectively. Note, that the separation of NPs is along the polarization axis of the incident field and the main part of energy is concentrated in the interparticle region. The field distribution in the gap between cubic nanoparticles is more uniform which is better from point of view DNA origami fluorescence study. However, other field distributions are also possible by changing the operating wavelength.

3. Conclusion

In summary, the plasmonic properties of a nanocube are much stronger compared to a nanosphere for both gold and silver particles. On the other hand, the LSPR and thus, sensitivity of the system can be increased by considering nanoparticle dimers. The analysis suggests the red shift of the resonant wavelength while decreasing the chamfering radius of corners of a cube and a field enhancement in the region between parts of a dimer. The field distribution in the gap between cubic nanoparticles is more uniform, which is better from point of view DNA origami fluorescence study, while in a nanosphere dimmer the field intensity is higher but distribution is nonuniform. Nonetheless, other distributions of electromagnetic field can also be achieved by considering some shift from resonant wavelengths.

4. Acknowledgments

This work was supported by the State Committee of Science of Armenia (grant No 16GE-027).

References

[1] S. Unser, I. Bruzas, Jie He and L. Sagle, "Localized surface plasmon resonance biosensing: current challenges and approaches Sensors," vol. 15, no 7, pp. 15684-15716, Jul. 2015.
[2] M. Hentschel,et al, "Linear and nonlinear optical properties of hybrid metallic–dielectric plasmonic nanoantennas," Beilstein J Nanotechnol, vol. 7, pp. 111–120, Jan. 2016.
[3] I. I. Slowing, Juan L.Vivero-Escoto,Chia-WenWu, Victor S.-Y.Lin, "Mesoporous silica nanoparticles as controlled release drug delivery and gene transfection carriers," Advanced drug delivery reviews, vol. 60, no. 11, pp. 1278-1288, Aug. 2008.
[4] I. Brigger, C. Dubernet, P. Couvreur, "Nanoparticles in cancer therapy and diagnosis," Advanced drug delivery reviews, vol. 60, pp. 24-36, Dec. 2012.
[5] V. Amendola, et al, "Surface plasmon resonance in gold nanoparticles: a review," Journal of Physics: Condensed Matter, vol. 29, no. 20, pp. 203002, Apr. 2017.
[6] M. Jahn, et al, "Plasmonic nanostructures for surface enhanced spectroscopic methods," Analyst, vol. 141, no. 3, pp. 756-793, Dec. 2015.
[7] S. Chen, M. Svedendahl, M. Käll, L. Gunnarsson and A Dmitriev, "Ultrahigh sensitivity made simple: nanoplasmonic label-free biosensing with an extremely low limit-of-detection for bacterial and cancer diagnostics," Nanotechnology, vol. 20, no. 43, pp. 434015, Oct. 2009.
[8] T. K. Sau and C. J. Murphy, "Room temperature, high-yield synthesis of multiple shapes of gold nanoparticles in aqueous solution," Journal of the American Chemical Society, vol. 126, no. 28, pp. 8648-8649, Jul. 2009.
[9] A. S. D. S. Indrasekara, S. Meyers, S. Shubeita, L. C. Feldman, T. Gustafsson and L. Fabris, "Gold nanostar substrates for SERS-based chemical sensing in the femtomolar regime," Nanoscale, vol. 6, no. 15, pp. 8891-8899, May. 2014.
[10] M. Thiele, A. Knauer, D. Malsch, A. Csáki, Th. Henkel, J. M. Köhlerb and W. Fritzsch "Combination of microfluidic high-throughput production and parameter screening for efficient shaping of gold nanocubes using Dean-flow mixing," Lab on a Chip, vol. 17, no. 8, pp. 1487-1495, May. 2017.